

## Numerical Simulation of Hydraulics and Heat Transfer in the BREST-OD-300 LFR Fuel Assembly

D.Fomichev<sup>1</sup>, D.Afremov<sup>1</sup>, A. Tutukin<sup>1</sup>, V.Smironov<sup>1</sup>, K.Sergeenko<sup>1</sup>

<sup>1</sup>JSC N.A. Dollezhal Research and Development Institute of Power Engineering (JSC NIKIET), Moscow, Russian Federation

*E-mail contact of main author: fomichev@nikiet.ru*

**Abstract.** In this paper, the results of numerical simulation of fluid dynamics and heat transfer in lead coolant flow through a central zone fuel assembly of the BREST-OD-300 reactor using CFD codes are presented. The commercial code STAR-CCM+ 10.02.010 and the LOGOS code developed by FSUE RFNC-VNIIEF (Sarov, Russia) were selected as the CFD codes.

For this investigation, nominal operating conditions of the fuel assembly were selected, corresponding to normal operating conditions of BREST-OD-300.

The numerical simulation was carried out in stationary RANS formulation. For turbulence models, Realizable  $k-\varepsilon$  (STAR-CCM+ 10.02.010) and SST  $k-\omega$  (LOGOS) models were selected.

Estimated values of flow characteristics (total pressure, velocity, temperature) are dimensionless and normalized to the corresponding maximum values. Agreement is shown between the estimated values and the experimental data, and the data obtained using the existing empirical correlations as well.

**Key Words:** BREST-OD-300, Fuel Assembly, CFD.

### 1. Introduction

Investigation of fluid dynamics and heat transfer of liquid metal coolant (LMC) flow in fuel assemblies (FAs) is one of the key objectives when validating the thermophysical reliability of the FA design and of the reactor core as a whole.

Currently, the development of computation technologies makes it possible to carry out such validations using computational fluid dynamics tools (i.e., CFD codes).

This paper aims at demonstration of CFD code application to the analysis of fluid dynamics and heat transfer in the lead coolant flow through the central zone (CZ) FA of BREST-OD-300 [1], and at determination of hydraulic and heat transfer characteristics of the flow and their comparison both to the experimental data, and to the data obtained using the existing empirical correlations.

### 2. Brief description of FA

The shroudless FA of BREST-OD-300 is comprised of a top nozzle, a bottom nozzle, the control mechanism of a bottom nozzle's positioning device and a bundle of smooth container-type fuel elements arranged in a triangular lattice. The control mechanism of the positioning device is designed to provide coupling and to transfer force from the gripper of a refueling machine to the spacer of the bottom nozzle. Spacing and positioning of the fuel elements are provided by nine honeycomb-type grids. Pitch-to-diameter ratio of fuel elements,  $p/d$ , is 1.38.

Relative spacer grid pitch,  $T/d$ , varies within a range of 21.0...33.0. Main geometrical parameters of FA are presented in Table I.

TABLE I: FA MAIN GEOMETRICAL PARAMETERS

Parameter	Value
Pin heated length, $L_{heat}$ , mm	1100
Pitch-to-diameter ratio, $p/d$	1.38
Hydraulic diameter of hexagonal flow channel, $d_{h,bdl}$ , mm	9.71
Hydraulic diameter of inner sub-channel, $d_{h,sch}$ , mm	10.71
Solidity of grid spacer, $e_{sp}$	0.14

### 3. Pressure loss coefficient and heat transfer correlations

This paper presents a comparison of the estimated data with the data obtained using the existing empirical correlations for determination of frictional resistance coefficients for a fuel bundle,  $\zeta$ , and a spacer grid,  $\zeta_{sp}$ , and with the data obtained using the generalized correlation between the Nusselt number, Nu, and the Peclet number, Pe, as well.

The frictional resistance coefficient of the bundle with smooth fuel rods arranged in the triangular lattice in the longitudinal coolant flow is defined as follows [2]

$$\zeta/\zeta_0 = 0.57 + 0.18 \cdot (p/d - 1) + 0.53 \cdot [1 - \exp(-a)],$$

where  $a = 0.58 + \{1 - \exp[-70 \cdot (p/d - 1)]\} + 9.2 \cdot (p/d - 1)$ ;  $\zeta_0 = 0.316 \cdot \text{Re}^{-0.25}$  is the frictional resistance coefficient for a round tube, while  $d_h = d_{h,sch}$ . Range of applicability of this correlation is  $\text{Re} = 2 \cdot 10^4 \dots 2 \cdot 10^5$  and  $p/d = 1.0 \dots 10.0$ .

Resistance coefficient of the spacer grid is expressed as a product of the two values [3]:

$$\zeta_{sp} = e_{sp}^m \cdot C_v,$$

where  $e_{sp} = A_p/A_{bdl}$  is ratio between the project cross section of the spacer grid to the bundle cross section;  $A_p$  is the project cross section of the grid;  $A_{bdl}$  is the total flow area of the fuel bundle;  $m = 0.2$ .

The  $C_v$  coefficient is determined from [3]

$$C_v = 1.104 + 791.8/\text{Re}^{0.748} + 3.348 \cdot 10^9/\text{Re}^{5.652},$$

where the Reynolds number is given by  $\text{Re} = G/A_{bdl} \cdot d_{h,bdl}/\mu$ .

The Nusselt number, Nu, is determined from the generalized correlation [4]

$$\text{Nu} = 0.047 \cdot (1 - \exp[-3.8 \cdot \{p/d - 1\}]) \cdot (\text{Pe}^{0.77} + 250),$$

where the Peclet number is given by  $\text{Pe} = (G/A_{bdl}) \cdot (d_{h,sch} \cdot c_p/\lambda)$ .

#### 4. CFD model description

A computational CFD-model of CZ FA is an FA structure surrounded by a hexagonal prism, which faces correspond to periodicity planes in accordance to the position of FA in the core reactor. The computational model includes the areas where the lead coolant enters (inlet) and leaves (outlet) the FA, respectively. The inlet area is cylindrical, its diameter is 360 mm and the height is 650 mm. The outlet area has a hexagonal cross-section and is 500 mm high. In the bottom nozzle region, the computational model is limited by the geometry of the reactor core support plate.

When generating the mesh model, a polyhedral-type mesh was selected. The mesh sensitivity analysis was carried out using different FA components: the top nozzle, the bottom nozzle and the fuel bundle with one spacer grid. The meshes selected based on the analysis results were used to generate the complete mesh model of the FA. The total amount of control volumes of the mesh is  $\sim 220$  millions, with approximately 65% of all control volumes assigned to the fuel bundle. The average dimensionless distance from the wall to the first control volume,  $y^+$ , is  $\sim 50$ .

The numerical simulation was carried out using two CFD-codes: the commercial CFD code STAR-CCM+ 10.02.010 and the in-house LOGOS code [5, 6], developed by FSUE RFNC-VNIIEF (Sarov, Russia).

Fluid dynamics and heat transfer in the FA were simulated in the stationary RANS formulation. For closing turbulence models, Realizable  $k-\varepsilon$  (STAR-CCM+) and SST  $k-\omega$  (LOGOS) models were selected. As a comment, it should be noted that the turbulent Prandtl number,  $Pr_t$ , was taken as a constant value equal to 0.9.

For the boundary conditions, the following parameters were adopted: lead coolant mass flow,  $G$ , and temperature,  $T$ , at the inlet of computational model, having a nominal value when the reactor operates under the normal operating conditions, and zero relative static pressure at the outlet of computational domain. For the corresponding opposite faces of the computational model, conditions of coolant flow periodicity were specified.

To account for the convective heat transfer at the outer surface of the fuel elements, a constant heat flux,  $q_w$ , of  $10^6$  W/m<sup>2</sup> was specified.

Given the specified boundary conditions, the typical Reynolds number,  $Re$ , for the lead coolant flow in the fuel bundle of CZ FA is  $\sim 9.5 \cdot 10^4$ , and the Peclet number,  $Pe$ , is  $\sim 1500$ .

The thermophysical properties of the lead coolant were given as functions of temperature (Table II) [7].

TABLE II: THERMOPHYSICAL PROPERTIES OF LEAD COOLANT AS A FUNCTION OF TEMPERATURE

Parameter	Functional expression
Density, $\rho$ , kg/m <sup>3</sup>	$(11.42 - 12.42 \cdot 10^{-4} \cdot T) \cdot 10^3$
Heat capacity, $c_p$ , J/(kg·K)	147.3
Thermal conductivity, $\lambda$ , W/(m·K)	$15.8 + 108 \cdot 10^{-4} \cdot (T - 600.4)$
Kinematic viscosity, $\nu$ , m <sup>2</sup> /s	$(15.87 \cdot 10^3 / T - 2.65) \cdot 10^{-8}$

## 5. Results

Fig.1 shows the distribution of dimensionless total pressure,  $p_{tot}$ , along the height of the FA computational model. Total pressure drop at the FA corresponds to the mentioned earlier drop across the reactor core within the framework of the reactor engineering design. The ratio between the total pressure drop at the bottom nozzle of the FA and the drop at the fuel portion is 0.28, and as for the top nozzle - 0.18. The specified ratios of total pressure drops in the hydraulic regions of the FA are in complete agreement with the experimentally obtained values.

The additional fluid dynamics analysis of the fuel portion was performed using the hydraulic frictional resistance coefficients of the fuel bundle,  $\zeta$ , and the hydraulic resistance of the spacer grid,  $\zeta_{sp}$  (Table III).

TABLE III: HYDRAULIC PARAMETERS OF FUEL BUNDLE

Parameter	Empirical correlations (see par. 3).	STAR-CCM+	LOGOS
Hydraulic frictional resistance coefficient of the fuel bundle, $\zeta$	0.0215	0.0210	0.0212
Deviation, $\Delta_{\zeta}$ , %	-	2.3	1.4
Hydraulic frictional coefficient of the spacer grid, $\zeta_{sp}$	1.010	0.74	0.75
Deviation, $\Delta_{\zeta_{sp}}$ , %	-	26.7	24.7

A significant discrepancy between the estimated values of the hydraulic frictional coefficient of the spacer grid and the data obtained from the empirical correlation results from the presence of the guide channels having a diameter larger than that of the fuel elements in the fuel bundle on the one hand, the absence of the FA's outer shroud on the other, and presence of bent elements in the peripheral rim of the spacer grid. Moreover, it should be noted that when determining the  $\zeta$  and  $\zeta_{sp}$  coefficients from the empirical correlations, the error is 15%.

Fig. 2 shows the distribution of total dimensionless pressure,  $p_{tot}$ , along the height of the CZ FA's computational domain normalized to the maximum total pressure (at the inlet to the FA computational domain). Analysis of total pressure,  $p_{tot}$ , distribution shows that there is an gradual pressure decrease. The pressure decrease,  $p_{tot}$ , at the spacer grids is periodic; starting from the second spacer grid, the loss of pressure is constant. The pressure loss at the first spacer grid is approximately 30% greater than that at the subsequent ones due to the non-stabilized flow when the coolant leaves the bottom nozzle and enters the FA fuel bundle.

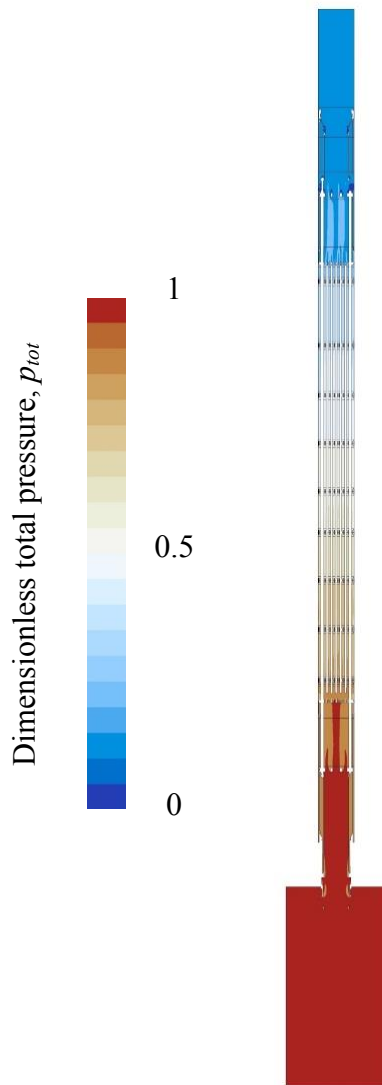


FIG. 1. Distribution of dimensionless total pressure of coolant over longitudinal section of CZ FA.

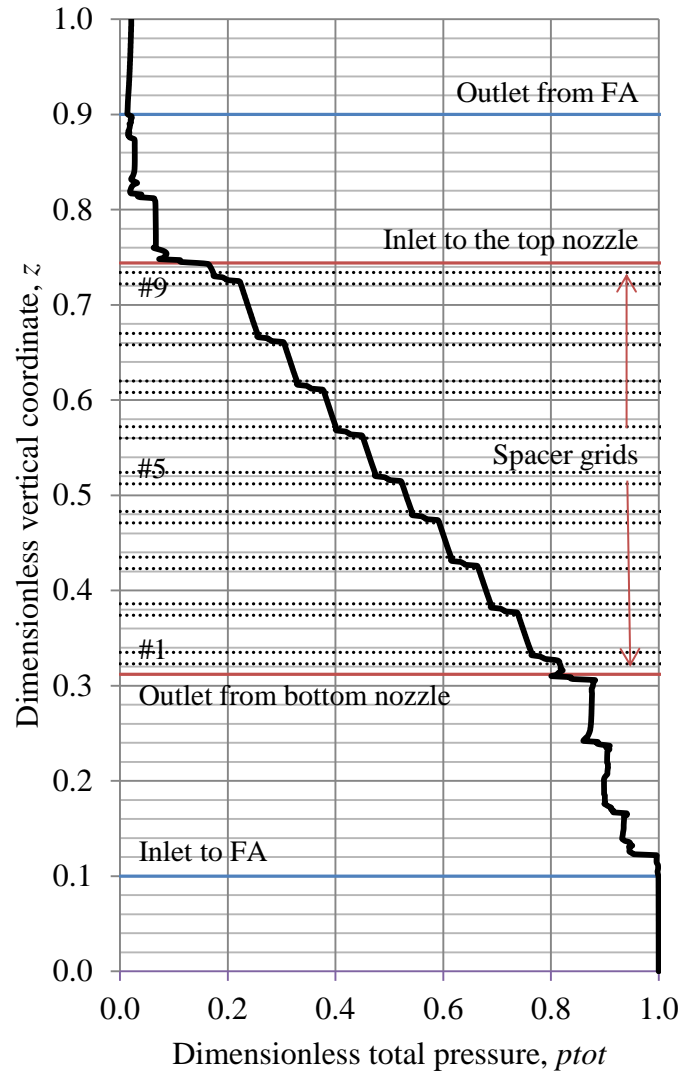


FIG. 2. Distribution of dimensionless total pressure of coolant along the height of CZ FA.

Fig. 3 shows the distribution of dimensionless velocity of the lead coolant in a flow direction,  $w$ , over the cross-section of the fifth spacer grid normalized to the maximum velocity across the said cross-section. The presence of bent elements in the peripheral rim of the spacer grid results in the considerable increase of the coolant flow velocity. The ratio between the average coolant flow velocity in the fuel bundle and the maximum velocity in the gap between the grids is  $\sim 1.8$ .

Fig. 4 shows the distribution of dimensionless temperature of the coolant in a flow direction,  $T$ , over the cross-section of the fifth spacer grid normalized to the maximum temperature across this cross-section.

Distribution of the coolant temperature over the FA cross-section corresponds to the specified power density conditions of the fuel elements. The maximum temperature values are within the acceptable design limits.

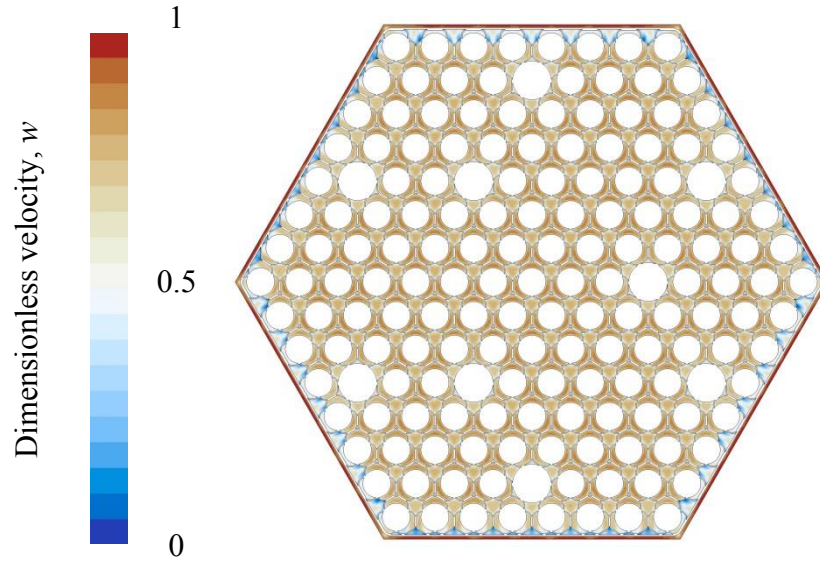


Fig. 3. Distribution of dimensionless coolant velocity of coolant over CZ FA cross-section.

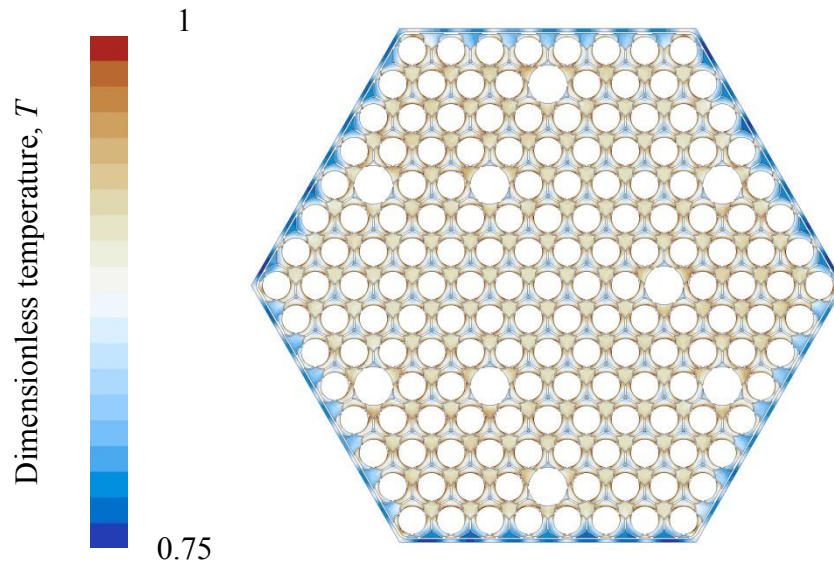


FIG. 4. Distribution of dimensionless temperature of coolant over CZ FA cross-section.

Comparison of the estimated Nusselt numbers,  $Nu$ , obtained for the fuel bundle area between the fifth and the sixth spacer grids is given in Table IV. Deviation of the estimated Nusselt numbers,  $Nu$ , obtained using the STAR-CCM+ and LOGOS CFD codes, from the values obtained using the empirical correlation (see par. 3) did not exceed 3%.

TABLE IV: HEAT TRANSFER PARAMETERS OF FUEL BUNDLE

Parameter	Empirical relationship (see par. 3).	STAR-CCM+	LOGOS
Nusselt Number, $Nu$	19.0	18.5	18.6
Deviation, $\Delta_{Nu}$ , %	-	2.6	2.1

## 6. Conclusions

This paper demonstrates the capability of both the commercial CFD code STAR-CCM+ and the in-house CFD code LOGOS to simulate fluid dynamic and heat transfer processes in the central zone FA of the BREST-OD-300 reactor. Both codes showed close values when estimating the hydraulic resistance coefficients of a fuel bundle and a spacer grid, and the Nusselt number in RANS formulation.

The estimated hydraulic characteristics of the the spacer grids differ from the values obtained using the empirical correlations. This is associated with the presence of the guide channels having a diameter larger than that of the fuel elements on the one hand, and with an absence of the FA's outer shroud on the other. The results also show a lack of a universal correlation for determination of the grid resistance coefficient. Good agreement found between hydraulic frictional resistance coefficient of the fuel bundle and the data obtained from the existing correlation.

Analysis of the heat transfer characteristics of the lead coolant flow in the FA indicated that although the turbulence models with a constant turbulent Prandtl number,  $Pr_t$ , of 0.9 were used, the deviation of the estimated Nusselt numbers,  $Nu$ , from the empirical values did not exceed 3%.

Finally, it may be concluded that the results of this paper demonstrate a principle possibility of numerical simulation of an FA in a liquid heavy metal coolant flow, and that the possibility to apply CFD codes will enable the transition from the simulation of a single FA with periodic boundary conditions to the simulation of the whole reactor core in the nearest future.

## 7. References

- [1] DRAGUNOV, YU.G., et al., "Detailed design of the BREST-OD-300 reactor facility: development stages and justification", Proc. 4th Int. Sci. and Tech. Conf. "Innovative Designs and Technologies of Nuclear Power", Book of Papers, Vol. 1, JSC NIKIET, Moscow (2016).
- [2] KIRILLOV, P.L., et al. "Nuclear power thermal-hydraulic analysis handbook. Volume 1. Thermal-hydraulic processes in NPP", Moscow, IzdAt, (2010) (In Russian).
- [3] PACIO, J., et al. "Heat transfer to liquid metals in a hexagonal rod bundle with grid spacers: Experimental and simulation results", Nuclear Engineering and Design (2015) 290, 27–39.
- [4] MIKITYUK, K. "Heat transfer to liquid metal: Review of data and correlations for tube bundles", Nuclear Engineering and Design (2009) 239, 680–687.
- [5] KOZELKOV, A.S., et al. "Multifunctional LOGOS software package: physical and mathematical models for computing aerodynamics, fluid dynamics and heat transfer", preprint 111-2013, Russia, Sarov, FSUE RFNC-VNIIEF (2013) (In Russian).
- [6] MELESHKIN, N.V., et al. "Verification of LOGOS software package for modeling of liquid metal coolant flow in fast reactor components", Innovations in nuclear power 2015 (Proc. Youth Conf. Moscow, 2015), Russia, Moscow, JSC NIKIET (2015) 261-272 (In Russian).
- [7] KIRILLOV, P.L., et al. "Nuclear power thermal-hydraulic analysis handbook. Volume 3. Thermal-hydraulic processes in transient and non-standard conditions. Severe accidents. Containment. Codes, their capabilities, uncertainties", Moscow, IzdAt, (2014) (In Russian).